Chapter 15
The Influence of Energetic Particles on the Chemistry of the Middle Atmosphere

Thomas Reddmann, Bernd Funke, Paul Konopka, Gabriele Stiller, Stefan Versick, and Bärbel Vogel

Abstract Energetic particle precipitation (EPP) during solar and geomagnetic active periods causes chemical disturbances in the lower thermosphere and in the middle atmosphere. Additional HO_x (H, OH, HO_2) and NO_x (N, NO, NO_2) are produced in the middle atmosphere, and enhancements of NO_x produced in these events can be transported to the winter stratosphere. These trace species take part in ozone chemistry and, by chemical-radiative coupling, the dynamical state in the middle atmosphere can be altered. There is evidence both from observations and from chemistry-climate models that the EPP induced signal in the middle atmosphere may then propagate into the troposphere. Thus particle precipitation could connect to possible climate effects. The first step in this functional chain is the impact of EPP on the chemical composition in the middle atmosphere and lower thermosphere, and the downward transport in the polar winter middle atmosphere. The general objective of this project was to assess quantitatively the chemical composition change in the middle atmosphere by combining model simulations and observations. The study relays mainly on the observations of the MIPAS instrument on the ENVISAT satellite, whose data set has been expanded in the context of this project by a newly developed retrieval of the gas H_2O_2, a reservoir for the members of the HO_x family. Simulations have been carried out with the two chemical transport models CLaMS and KASIMA, which cover chemistry and transport effects in the stratosphere up to the mesosphere/lower thermosphere region. The impact on the global NOy budget

T. Reddmann (✉) · G. Stiller · S. Versick
Karlsruhe Institute of Technology (KIT), Inst. for Meteorology and Climate Research, Karlsruhe, Germany
e-mail: thomas.reddmann@kit.edu

P. Konopka · B. Vogel
Institute for Energy and Climate Research – Stratosphere (IEK-7) Forschungszentrum Jülich GmbH (FZJ), Jülich, Germany

B. Vogel
e-mail: b.vogel@fz-juelich.de

B. Funke
Instituto de Astrofisica de Andalucia (CSIC), Granada, Spain
e-mail: bernd@iaa.es

F.-J. Lübken (ed.), *Climate and Weather of the Sun-Earth System (CAWSES)*,
Springer Atmospheric Sciences,
DOI 10.1007/978-94-007-4348-9_15, © Springer Science+Business Media Dordrecht 2013

and (the resulting) total ozone change are assessed in these studies. In addition, the ion reaction mechanism for the conversion of N_2O_5 to HNO_3 based on positive ion chemistry was refined. The detailed comparison of model results and observation for the SPE 2003 showed that models can simulate the impact of EPP on ozone chemistry but deficiencies exist for some minor species.

15.1 Introduction

The interaction of solar coronal mass ejections and the solar wind with the interplanetary plasma and processes in the Earth's magnetosphere accelerate particles as protons, electrons, or He nuclei to energies up to the GeV range. Some of these energetic particles penetrate the atmosphere mainly at high geomagnetic latitudes and lose their kinetic energy by cascades of inelastic collisions. Via ionization, dissociation and ion reactions this energy deposition ultimately produces reactive molecules like NO, NO_2, OH and others. This significant enhancement of NO_x ($= NO + NO_2 + N$) and HO_x ($= H, OH, HO_2$) causes additional ozone loss and disturbs other trace gas distributions.

During polar night and the absence of photochemistry the impact of energetic particle precipitation (EPP) on the chemical state of the atmosphere is most pronounced per se. But the interhemispheric diabatic circulation with its downward branch in the polar winter hemisphere in addition allows to propagate the result of this interaction, which mainly takes part in the thermosphere and mesosphere, to the stratosphere. The key processes for the impact of EPP on the middle atmosphere are therefore the combination of disturbed chemistry and transport in the winter polar middle atmosphere.

After its maximum in the year 2000/2002 the solar cycle 23 exhibited prolonged activity which gave rise to several extraordinary manifestations of solar-terrestial connections in the Earth's middle atmosphere. Several strong flare events and several strong geomagnetic storms were responsible for remarkable chemical disturbances in the middle atmosphere in both hemispheres. Evidence for regular long range NO_x descent had already been observed in several satellite experiments [*Callis et al.*, 1996; *Randall et al.*, 1998, 2001; *Rinsland*, 1996], for example from the Halogen Occultation Experiment (HALOE) instrument on UARS, and from the ATMOS and POAM experiments. The late solar cycle 23 fell in a period where new and most capable instruments on satellites gave a wealth of new information for these processes, i.e. the instruments for the determination of atmospheric composition on the ENVISAT satellite, launched in early 2002, SCIAMACHY, GOMOS and MIPAS, the instrument ACE FTS, MLS on Aura, Odin's SMR instrument. The new observational results offered the possibility for detailed and comprehensive model studies to test and improve our understanding of chemical and dynamical processes in the middle atmosphere as a whole. Together with the exceptional active sun, the conditions to study EPP related processes were excellent.

Since July 2002, the Michelson Interferometer for Passive Atmospheric Sounding (MIPAS) onboard the satellite ENVISAT of the European Space Agency (ESA)

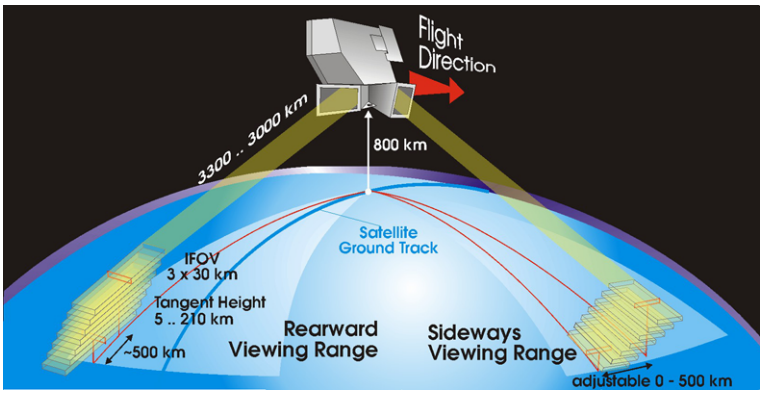

Fig. 15.1 Observation scheme of the MIPAS instrument on the ENVISAT satellite (source ESA)

observes the middle atmosphere from the upper troposphere up to the mesosphere. In Fig. 15.1 a schematic view of MIPAS in space is shown, focusing on observation modes. MIPAS is a Fourier transform spectrometer for the measurement of high-resolution gaseous emission spectra at the Earth's limb [*Fischer and Oelhaf*, 1996; *Fischer et al.*, 2008]. It allows to retrieve global distributions of trace gases as for example O_3, HNO_3, CH_4, N_2O and many other substances. These observations represent one of the most complete data sets for studying the influence of energetic particle induced changes in the middle atmosphere as they cover the middle atmosphere during polar night. This is an important advantage of the MIPAS/ENVISAT dataset compared to other observations, e.g. from UV-VIS instruments or from solar occultation instruments, which both depend on solar light. Reactive and reservoir gases, and tracers for the transport in the polar winter middle atmosphere are included in the dataset. Figure 15.2 shows as an example the time series of NO_2 night-time observations derived from an operational MIPAS data-product provided by ESA (see next paragraph).

Data are available for example from the operational ESA level 2 MIPAS/ENVISAT data product. An advanced data record with more substances and also dealing with non-LTE effects, has been generated at the Institute for Meteorology and Climate Research—Atmospheric Trace Gases and Remote Sensing at KIT and the Instituto de Astrofisica de Andalucia (CSIC) (see *Lacoste-Francis* [2010]). By now, this advanced data record contains more than 20 substances and spans the period from July 2002 to 2010. From July 2002 to March 2004 MIPAS observed with a spectral resolution of 0.025 cm^{-1}, afterwards the spectral resolution was reduced, but the vertical resolution improved [*von Clarmann et al.*, 2009]. MIPAS could observe in detail the solar storms of October/November 2003 known as 'Halloween' storms as well as NO_x intrusions in the years 2004 and 2009 in the NH, observations which gave rise to the detection of new effects related with EPP as documented in a number of publications [*Jackman et al.*, 2005, 2008; *Orsolini et al.*, 2005; *Lopez-Puertas et al.*, 2005a, 2005b; *Funke et al.*, 2005, 2008; *von Clarmann et al.*, 2005].

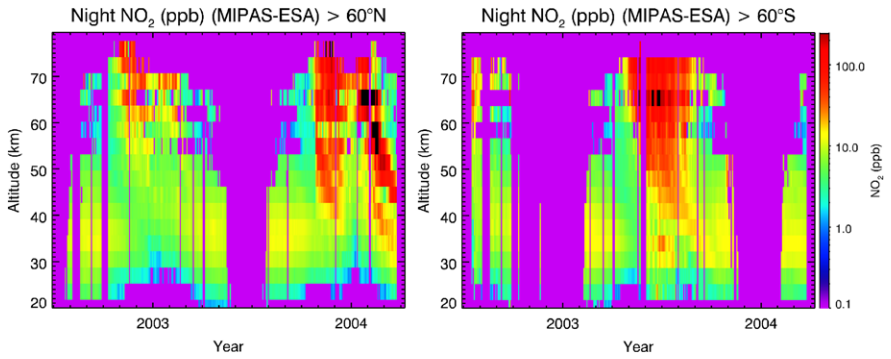

Fig. 15.2 NO_2 night-time observations of the MIPAS instrument on the European ENVISAT satellite, (**a**) Northern hemisphere, (**b**) Southern hemisphere between July 2002 and March 2004. In the NH the weak (2002/3) and strong (2003/4) intrusion from the mesosphere/lower thermosphere are seen together with the NO_x enhancement after the Halloween storms in November 2003, in the SH the pronounced intrusion from the MLT in the course of the Antarctic winter can be seen (from *Reddmann et al.* [2010], reproduced by permission of American Geophysical Union)

In several model studies principal effects of EPP have been studied in the past (e.g. *Siskind et al.* [2000], see *Jackman and McPeters* [2004] for an overview of related work). 3D-model studies of the effects of EPPs have been performed with chemistry climate models (CCMs) applying artificial NO_x enhancements [*Langematz et al.*, 2005; *Rozanov et al.*, 2005] or modules calculating NO_x and HO_x production from prescribed ionization rates (e.g. *Jackman et al.* [2008]). *Baumgaertner et al.* [2009] adapted results of *Randall et al.* [2007] to estimate effects of NO_x produced by low energy electrons in the middle atmosphere. Many model simulations qualitatively reproduce various effects connected with EPPs, but the necessary tight connection of chemical disturbances and transport is still a challenge for current 3D-models of the middle atmosphere. Model simulations using actual meteorological conditions comparing their results with corresponding observations are therefore a valuable tool to test our understanding of the relevant processes in these events. This project focuses on such comparisons.

The first approach within the project to assess the effects caused by EPP was to use detailed observations, primarily of the MIPAS instrument on the ESA satellite ENVISAT, as a boundary condition for the additional NO_x in model simulations. Two chemical transport models took part in this approach, the CLaMS and the KASIMA model. The observations of MIPAS used for the studies cover the period from July 2002 till March 2004 and include the Antarctic winter 2003 with strong NO_x enhancements originating in the upper mesosphere and lower thermosphere, the strong SPE event and the following geomagnetic storms (Halloween storms) in October/November 2003, and the NO_x intrusion following a stratospheric warming in Arctic mid-winter 2003/2004. From these simulations the effect on ozone chemistry could be deduced, e.g. the additional ozone loss and changes in other chemical substances could be quantified. Some results of this work are presented in Sect. 15.2, details can be found in *Vogel et al.* [2008] and *Reddmann et al.* [2010].

The second approach concentrated on the solar proton event in October/November 2003 and had therefore the direct effects of the EPP-atmosphere interaction in the focus, e.g. the amount of produced NO_x and HO_x, and changes of several substances in a short period during and after the ionization event. The very comprehensive observations of the MIPAS instrument of the species NO, NO_2, H_2O_2, O_3, N_2O, HNO_3, N_2O_5, HNO_4, ClO, HOCl, and $ClONO_2$, CO, CH_4, and H_2O allow a profound test of the chemistry implemented in models together with their transport properties in the polar winter middle atmosphere. An international model-data intercomparison project (High Energy Particle Precipitation in the Atmosphere, HEPPA) was established including both chemical transport models, and chemistry-climate models [*Funke et al.*, 2011]; of the nine participating models, five were also involved in the CAWSES SPP, as was the derivation of ionization rates with the AIMOS model (see also Chaps. 9 and 13). The HEPPA intercomparison initiative has lately been invited to become part of the SPARC SOLARIS initiative. For these comparison, the KASIMA model was extended to include a module for NO_x and HO_x production by ionizing particles. Ionization rates have been calculated within the KASIMA model or using the precalculated ionization rates provided by the AIMOS calculations (*Wissing and Kallenrode* [2009], see also Chap. 13. A short overview of results for the KASIMA model is given in Sect. 15.3, for details see *Funke et al*. [2011]).

Rather few observations exist which show the effects of EPP for the HO_x family [*Verronen et al.*, 2006]. Whereas the long-term effects of EPP produced HO_x are probably small, HO_x related fast reactions during the particle interaction seem to be the least understood in the models. A new retrieval setup for MIPAS/ENVISAT observations was therefore developed to assess possible enhancements of H_2O_2 after EPP. H_2O_2 serves as a reservoir of HO_x and it was expected that H_2O_2 concentrations should be enhanced during and after SPEs, and could indeed be detected by the new retrieval scheme. A climatology of H_2O_2 and EPP related enhancements is presented in Sect. 15.4. These data were also used as an additional species in the HEPPA intercomparison.

A strong impact on the partitioning within the NOy family has been observed when NO_x intrusions reach the upper stratosphere resulting in a secondary maximum of HNO_3 distribution in th upper stratosphere [*Kawa et al.*, 1995; *Stiller et al.*, 2005]. The proposed conversion of N_2O_5 to HNO_3 can be explained via a mechanism involving protonized water vapor clusters. A new parameterization was developed within the project for this reaction, and it was found that this conversion may have also an impact in the lower stratosphere. The inclusion of this reaction gives better agreement between HNO_3 observations and model results there (see Sect. 15.5).

Finally, the observations and model results clearly showed that not the strong but rare SP events are the main contributors to EPP related NO_x in the middle atmosphere, but the seemingly more regular but weaker auroras and geomagnetic storms. Most probably, very efficient transport from the lower thermosphere is the key process for these dramatic NO_x enhancements. This efficient transport seems to be related to specific dynamic situations. This finding connects the rather restricted

study of chemical EPP effects to the more general question how the MLT region interacts with the lower atmosphere.

15.2 Model Studies with Imposed NO_x Disturbance

Within this project two different chemical transport models were applied to study the chemical effects of NO_x intrusions in the stratosphere, namely the CLaMS model and the KASIMA model. The models use a quite different model architecture and focus on different aspects. The Chemical Lagrangian Model of the Stratosphere (CLaMS) is a Lagrangian chemical transport model, which uses 3-dimensional deformations of the large-scale winds to parameterize mixing and is very well suited to study horizontal transport and mixing processes as shown in previous studies [*McKenna et al.*, 2002a, 2002b; *Konopka et al.*, 2007a]. KASIMA is a combination of a Euler model using analyzed winds in the lower domain, and a mechanistic model on top, and covers the vertical domain up to the lower thermosphere. It focuses on long-term transport processes including the mesospheric branch of the residual circulation and chemical processes in the middle atmosphere.

Both simulations show that the NO_x intrusions can have a significant impact on the ozone budget in the middle stratosphere maximizing in the middle stratosphere where additional ozone loss between 30 %–50 % is deduced. The effect on total ozone was found to be non-negligible but restricted to high latitudes within a range of about 10 DU.

15.2.1 The Arctic Winter 2003/4: The CLaMS Perspective

To study the impact of the downward transport of NO_x-rich air masses from the mesosphere into the lower stratosphere on stratospheric ozone loss, CLaMS simulations were performed for the Arctic winter 2003/04. This winter includes the Halloween storms at beginning of the winter in late October and the NO_x intrusions descending in late winter from the lower thermosphere/mesosphere to the stratosphere. In late December, a stratospheric warming occurred, and low latitude air masses were transported to high latitudes.

CLaMS is based on a Lagrangian formulation of the tracer transport and, unlike Eulerian CTMs, considers an ensemble of air parcels on a time-dependent irregular grid that is transported by use of the 3d-trajectories. The irreversible part of transport, i.e. mixing, is controlled by the local horizontal strain and vertical shear rates with mixing parameters deduced from observations (e.g. *Konopka et al.* [2003], *Grooß et al.* [2005]). CLaMS therefore is especially suited to study horizontal transport processes at the boundary of the polar vortex, and possible loss of the SPE or MLT enriched air masses by the mixing processes occurring during the stratospheric warming.

The simulations cover the altitude range from 350–2000 K potential temperature (approx. 14–50 km). The horizontal and vertical transport is driven by ECMWF winds and heating/cooling rates are derived from a radiation calculation. The mixing procedure uses the mixing parameter as described in *Konopka et al.* [2004] with a horizontal resolution of 200 km and a vertical resolution increasing from 3 km around 350 K potential temperature to approximately 13 km around 200 K potential temperature according to the model set up *Konopka et al.* [2007b]. The halogen, NO_x, and HO_x chemistry mainly based on the current JPL evaluation *Sander et al.* [2006] is included.

Before the first SPE has occurred, the model is initialized once at 4 October 2003 with mainly MIPAS observations (V3O) from 3–5 Oct 2003 (CH_4, CO, N_2O, O_3, NO, NO_2, N_2O_5, HNO_3, H_2O, and $ClONO_2$) processed at IMK and at the Instituto de Astrofisica de Andalucia (IAA), Granada, Spain. In the model, the flux of enhanced NO_x from the mesosphere is implemented in form of the upper boundary conditions at 2000 K potential temperature (50 km altitude) which are updated every 24 hours. The NOy constituents NO_x, N_2O_5, HNO_3 and the tracers CH_4, CO, H_2O, N_2O, and O_3 at the upper boundary are taken from results of a long-term simulation performed with the KASIMA model (Karlsruhe Simulation Model of the middle Atmosphere), see next section. In this KASIMA simulation, enhanced NO_x concentrations in the mesosphere during disturbed periods have been derived above 55 km from MIPAS observations (provided by the European Space Agency (ESA)).

In addition to this ClaMS reference model run (referred to as 'ref' run) a model simulation without an additional NO_x-entry at the upper boundary is performed. In addition, to estimate the possible maximum impact of NO_x on stratospheric ozone loss, we derive a maximum NO_x-entry at the upper boundary condition from several satellite measurements of NO and NO_2 by the MIPAS, HALOE, and ACE-FTS instruments. For each day at the upper boundary the NO_x mixing ratios for equivalent latitudes greater or equal 60°N are replaced by the maximum NO_x value observed by any satellite instruments within 60° and 90°N at 2000 K potential temperature at that day, respectively, by the maximum NO or NO_2 value if no NO_x measurement exists in this 24 hour period. For days where no satellite observations are available we take the maximum NO_x derived by KASIMA at that day. This model simulation is referred to as 'max NO_x' run.

Clams results of NOx enhancements and resulting ozone loss are shown for polar latitudes in Fig. 15.3. For the Arctic polar region (Equivalent Lat. $>70°$N) we found that enhanced NO_x caused by SPEs in Oct–Nov 2003 is transported downward into the middle stratosphere to about 800 K potential temperature ($\approx$30 km) until end of December 2003. The mesospheric NO_x intrusion due to downward transport of upper atmospheric NO_x produced by auroral and precipitating electrons [*Funke et al.*, 2007] affects NO_x mixing ratios down to about 700 K potential temperature ($\approx$27 km) until March 2004. A comparison of the reference run with a simulation without an additional NO_x source at the upper boundary shows that O_3 mixing ratios are affected by transporting high burdens of NO_x down to about 400 K (17–18 km) during the winter (see Fig. 15.3). Locally, an additional ozone loss of the order 1 ppmv is simulated for January between 850–1200 K potential temperature during the period of the strong polar vortex in the middle stratosphere.

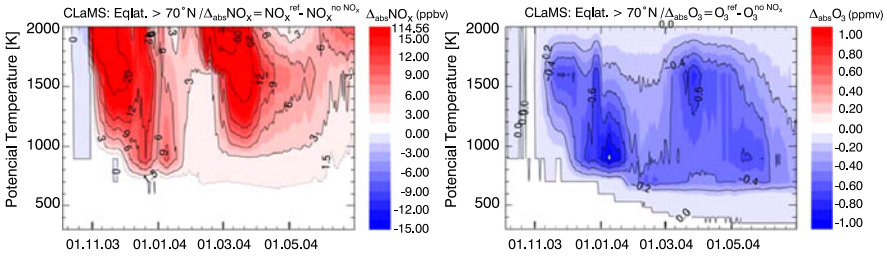

Fig. 15.3 Additional NO_x (ΔNO_x) and ozone reduction ΔO_3 poleward of 70°N equivalent latitude due to mesospheric NO_x intrusions over the course of the winter 2003–2004 for the reference model run (from *Vogel et al.* [2008])

An intercomparison of simulated NO_x and O_3 mixing ratios with satellite observations by ACE-FTS and MIPAS shows that the NO_x mixing ratios at the upper boundary derived from KASIMA simulations are in general too low (see Fig. 15.4). Therefore a model simulation with higher NO_x mixing ratios at the upper boundary derived from satellite measurements was performed. For this model run ('max NO_x') the simulated NO_x mixing ratios and the total area of enhanced NO_x mixing ratios are in general higher compared to satellite observations and so provide so an upper limit for the impact of mesospheric NO_x on stratospheric ozone chemistry. The comparison between simulated and observed ozone mixing ratios confirm the 'max NO_x' run is an upper limit which overestimates the NO_x entry at the upper boundary and underestimates O_3 due to stronger O_3 destruction. Moreover in the 'ref' run the simulated O_3 is in very good agreement with satellite measurements (see Fig. 15.4).

For the different runs ozone loss was calculated from the simulated O_3 values minus the passively transported ozone. Halogen-induced ozone loss plays a minor role in the Arctic winter 2003/2004 because the lower stratospheric temperatures were unusually high. Therefore the ozone loss processes in the Arctic winter stratosphere 2003/2004 are mainly driven by NO_x chemistry. Further, in addition to the transport of NO_x-rich mesospheric air masses in the stratosphere due to SPEs in Oct–Nov 2003 and the downward transport of upper atmospheric NO_x produced by auroral and precipitating electrons in early 2004, the ozone loss processes are also strongly affected by meridional transport of subtropical air masses. Likewise, in this case air masses rich in both ozone and NO_x are transported during the major warming in December 2003 and January 2004 into the lower polar stratosphere.

Our findings show that in the Arctic polar vortex (Equivalent Lat. $>70°$N) the accumulated column ozone loss between 350–2000 K potential temperature (~14–50 km) caused by the SPEs in Oct–Nov 2003 in the stratosphere is up to 3.3 DU with an upper limit of 5.5 DU until end of November (see Fig. 15.5). Further we found that about 10 DU but lower than 18 DU accumulated ozone loss additionally occurs until end of March 2004 caused by the transport of mesospheric NO_x-rich air in early 2004. In the lower stratosphere (350–700 K, approx. 14–27 km) the SPEs of Oct–Nov 2003 have negligible small impact on ozone loss processes until end of

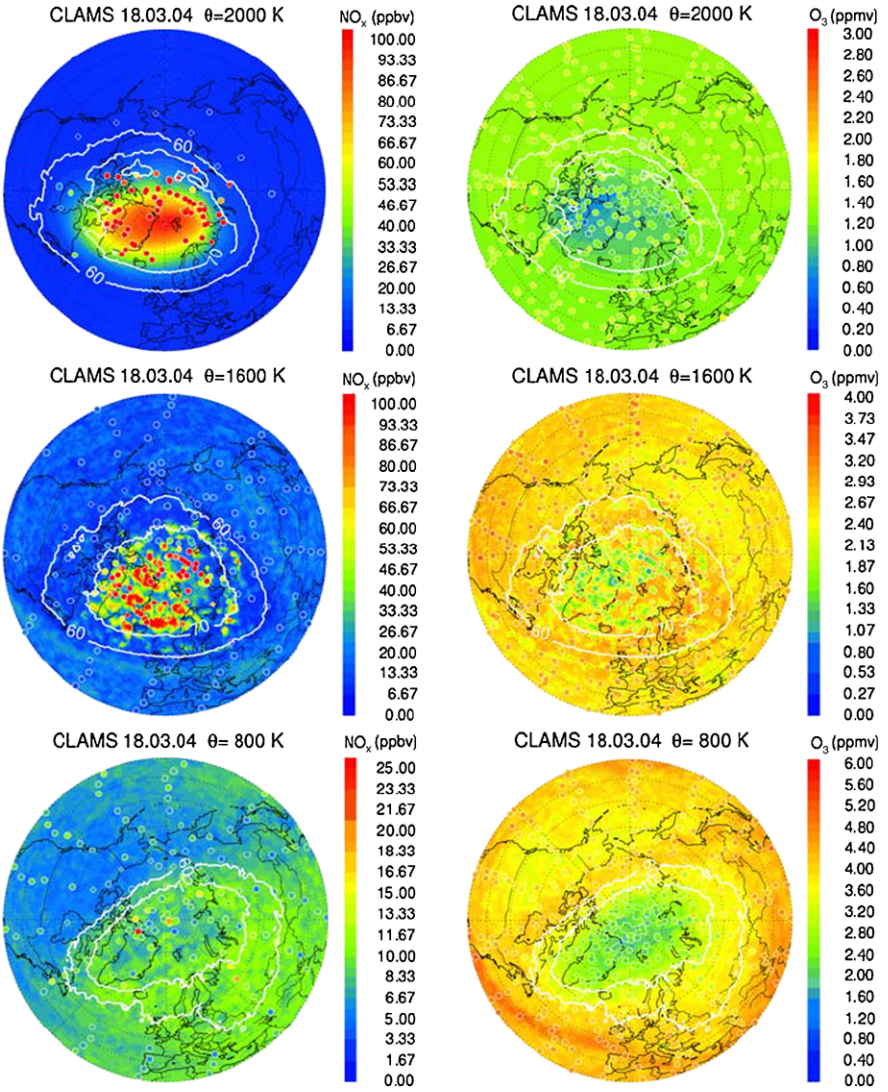

Fig. 15.4 Horizontal view of NO_x and O_3 at 2000 K, 1600 K, and 800 K potential temperature for the reference model run on March 18, 2004. The isolines for the equivalent latitude at 60°N and 70°N are marked by *white lines*. The model results and satellite observations (IMK/IAA-MIPAS: *circles* and ACE-FTS: *diamonds*) are shown for noon time. We note that all NO_x mixing ratios beyond the scale are also plotted in *red* (from *Vogel et al.* [2008])

November and the mesospheric NO_x intrusions in early 2004 yield ozone loss about 3.5 DU, but clearly lower than 6.5 DU until end of March. Overall, the downward transport of NO_x-rich air masses from the mesosphere into the stratosphere is an

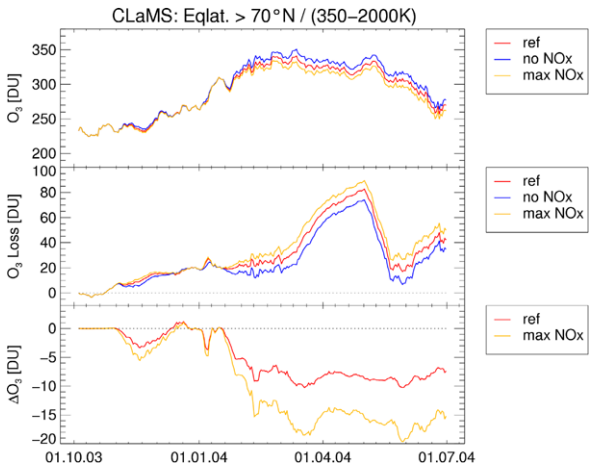

Fig. 15.5 Column ozone (in Dobson units) with (*red*), without (*blue*), and with a maximum (*yellow*) mesospheric NO_x sources integrated over the entire simulated altitude range from 350 K until 2000 K (∼14–50 km) for equivalent latitudes poleward of 70°N. *Middle panel*: Ozone loss in DU for these model runs. *Bottom panel*: ΔO_3 caused by the additional NO_x-source at the upper boundary. Shown is the ozone column of the 'no NO_x' run minus the ozone column of the 'ref' (*red*) and the 'max NO_x' run (*green*) (from *Vogel et al.* [2008])

additional and non-negligible variability to the existing variations of the ozone loss observed in the Arctic.

15.2.2 KASIMA Studies: The Period 2002–2004

The KASIMA model is a 3D mechanistic model of the middle atmosphere which can be coupled to specific meteorological situations by using analyzed lower boundary conditions and nudging terms for vorticity, divergence and temperature. The model is based on the solution of the primitive meteorological equations in spectral formulation and uses the pressure altitude as vertical coordinate. Its vertical domain spans the upper troposphere up to the lower thermosphere. In the MLT region, winds are calculated using physical parameterizations for heating rates and gravity wave drag based on a Lindzen scheme. The model has been used for investigations of transport and chemistry in the middle atmosphere [*Kouker*, 1993; *Reddmann et al.*, 1999, 2001; *Ruhnke et al.*, 1999; *Kouker et al.*, 1999; *Khosrawi et al.*, 2009]. The model simulates long-term transport in the stratosphere reasonably well. This has been shown by comparisons with the inert tracer SF_6 and derived mean age of air [*Engel et al.*, 2006; *Stiller et al.*, 2008].

The rationale of this model study was to use two model runs, one standard run, and one with a changed upper boundary condition for NO_x from EPP to derive its impact on the chemical state in the middle atmosphere. No feedback of the chemistry is included to the ozone field used for the calculation of heating rates in the run, so both simulations use the same dynamics for transport and allow to single

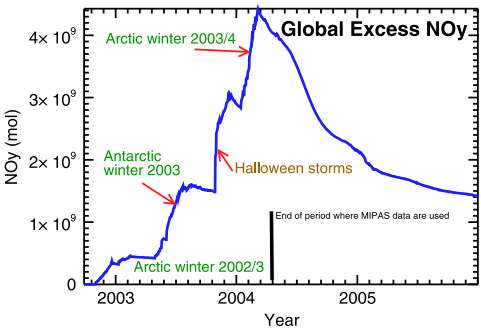

Fig. 15.6 Global excess NO_y from energetic particle production (from *Reddmann et al.* [2010]), modified by permissions of the American Geophysical Union)

out the change esp. of ozone for the disturbed chemical conditions. With a good representation of the mean transport times, the model can therefore be used to study the effects of NO_x intrusions on a longer time-scale. Against the background of the undisturbed stratosphere, the NO_x enhancements in the observations and in the model can be clearly traced as seasonal events restricted to polar latitudes, leaving the rest of the stratosphere mostly unaffected. This allows to estimate the chemical effects of NO_x intrusions by comparing the disturbed and the undisturbed model run, and to analyze the individual events which show different characteristics between intrusions starting in the upper mesosphere and the SPE with enhancements down to the stratosphere. Coupling effects between chemical changes due to EEPs and dynamics take place in the real atmosphere, and are therefore implicitly included in the dynamical fields used in the nudged model. In this sense, the chemical effects are also influenced by the coupling, as the reference dynamical state does not correspond to a real undisturbed one. Nevertheless, for the purpose of quantifying the strength of the NO_x intrusions on chemistry this is only an effect of minor importance.

For our study we used reprocessed operational MIPAS NO_2 data which had a nearly daily coverage [*Ridolfi et al.*, 2000; *Carli et al.*, 2004]. NO_x has a photochemical lifetime of a few days in the mesosphere and during night most of NO_x is in the form of NO_2. Nighttime observations of NO_2 are taken therefore as a representative for the concentration of NO_x.

Figure 15.2 shows time-height cross sections of the mean NO_2 volume mixing ratio of the northern and southern polar cap (geographical latitudes polewards of 60°) in ppb, from the ESA MIPAS/ENVISAT nighttime observations as described above. NO_x values from the MIPAS/ENVISAT observations using nighttime NO_2 as a proxy for NO_x, are imposed on the model values during times of diagnosed increased levels of NO_x in the polar mesosphere and during the SPE in October/November 2003. The ESA dataset has been preferred over other data sets based on MIPAS/ENVISAT observations as it provided a rather complete coverage for the MIPAS/ENVISAT phase I observation period, but it lacks the accuracy of the IMK-IAA data set as it does not include non-LTE effects and does not consider horizontal gradients of mixing ratios in the retrieval (see *Wetzel et al.* [2007]).

The sum of all inorganic nitrogen-containing species except N_2 and the source gases like N_2O is called NO_y, enhanced after EPP [*Brasseur and Solomon*, 2005].

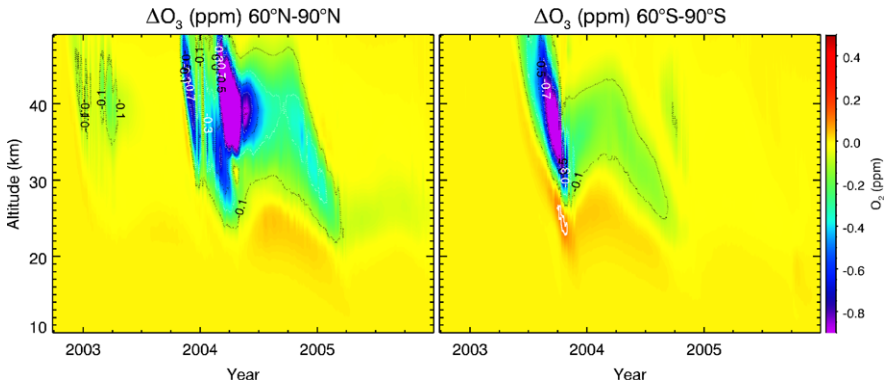

Fig. 15.7 Ozone change through EPP effects (from *Reddmann et al.* [2010], reproduced by permission of American Geophysical Union)

Figure 15.6 shows the global excess NO_y in mol for the period July 2002 to December 2005. The auroral winter intrusions in the Arctic winter 2002/2003 and Antarctic winter 2003, the SP event in fall 2003 and the strong intrusion in the Arctic winter 2003/2004 are clearly discernible as single events adding to the total NO_y background. The characteristic time-scale for the decay of the additional NO_y in the model lies in the range of about 2 years.

We estimate the additional NO_y in Arctic winter 2002/2003 at 0.4 Gigamol (GM), in Antarctic winter 2003 at about 1.4 GM, the NO_y from the SPE at about 1.5 GM and in January 2004 at about 2 GM. As in the Arctic winter both intrusions overlap, they cannot clearly be separated. The value estimated for the Antarctic winter 2003 is about 75 % of the value *Funke et al.* [2005] deduced from their observation based study with MIPAS/ENVISAT data. *Randall et al.* [2007] give a range of 1 to 2 GM estimated from HALOE observations for this winter, depending on the use of average or maximum observed NO_x values. Globally, the additional NO_y in the model which we derive amounts at its maximum to about 5 % of the total 70 GM NO_y in the middle atmosphere from the oxidation of N_2O.

The effects of the additional NO_y in the atmosphere on the formation of particles in the cold polar vortex (for example by changing the saturation vapor pressure) is small, but still significant. The mass of NO_y in NAT-particles increases in the Antarctic winter 2004 and the Arctic winter 2004/2005 by about 5 %.

Figure 15.7 shows the effects on ozone for the whole simulation period again for 75°S and 75°N. Additional ozone loss lasts for the following year in the Southern Hemisphere at the level of about 0.2 ppm. At the end of 2004 a small ozone change can be found above the band related to the Antarctic winter 2003. Closer inspection of time-latitude cross sections of NO_y at different altitudes show that during summer 2004 NO_y is transported from the Northern to the Southern Hemisphere at the stratopause level (not shown) exceeding 1 ppb, causing the additional ozone loss. During the Arctic winter 2002/2003 the minor amounts of additional NO_x cause only small ozone changes. The maximum changes occur during spring 2004, exceed 30 % and follow closely the downward transport of the additional NO_x. The

changes caused by the SPE in fall 2003 can be traced until spring 2004 below 30 km but are lost to lower latitudes. The enormous amounts of additional NO_x from January cause ozone changes of several percent even in the following spring at altitudes of about 30 km.

The NO_x induced additional ozone loss causes also changes in total ozone. In the Southern Hemisphere ozone changes are restricted to the Antarctic region. In the Northern Hemisphere a decrease of total ozone of several Dobson units reach the mid-latitudes. At high latitudes changes of about 5 DU can be found even in spring 2005.

15.3 The Solar Proton Events of Oct/Nov 2003 and Direct Effects

This section deals with the second approach where HO_x and NO_x enhancements are calculated in the models directly from ionization rates. This allows chemistry climate models to include EPP effects as a function of solar and geomagnetic activity. The role of CTMs is here again to validate the results of such calculations with the help of detailed observations. Within the CAWSES project the KASIMA model was expanded to include these direct effect using particle flux data from satellites as GOES. Again, the very well observed HALLOWEEN storms have been used to make these comparisons using the MIPAS data set. These comparisons were carried out in the framework of an international model measurement intercomparison initiative of CCMs and CTMs [*Funke et al.*, 2011]. For KASIMA as for most of the other models taking part in that inter-comparison the general agreement between observations and model is reasonable but by far not perfect.

As the HO_x cycle is not well represented in observations a new retrieval strategy was implemented in the MIPAS analysis to derive H_2O_2 concentrations in the middle atmosphere. For the first time, a H_2O_2 climatology could be derived and enhancements during the SPE effect in 2003 could be observed. The comparison with the model shows a qualitative but not a quantitative agreement, hinting at deficits of our understanding of the chemical processes related to H_2O_2 in general as well as and in particular during and after atmospheric ionization events.

15.3.1 Ionization Rates and HO_x and NO_x Production

Different kind of particles contribute to the ionization in the atmosphere. Enhanced fluxes of energetic protons can be included in models with reasonable accuracy by an approximate description, for example applying the Bethe-Bloch formula and assuming that the protons fill the geomagnetic polar cap more or less homogeneously, as it is the case for solar proton events. The spectral flux distribution of the protons has to be derived from measurements of particle detectors on satellites (GOES data series) which only give integrated counts for a few channels. In KASIMA we applied a particle flux of the form $J(E) = A \cdot E^{-\delta}$, where A and δ have been derived

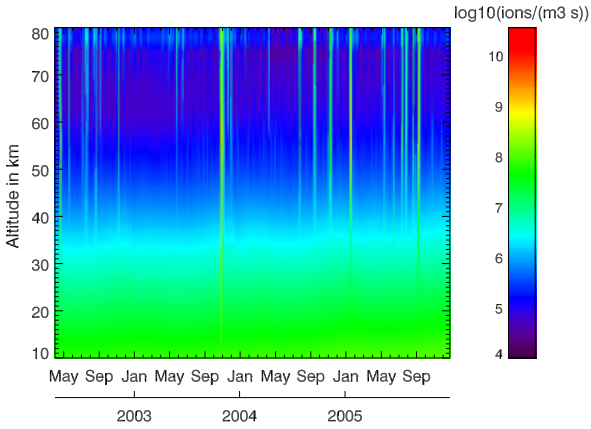

Fig. 15.8 Ionization rate from protons and cosmic rays calculated in the KASIMA SPE module (from *Versick*, 2011)

by a fit procedure (see *Versick* [2011]). We also included a component from cosmic rays using the formalism of *Heaps* [1978]. Figure 15.8 shows ionization rates calculated as described above. It shows distinct and sporadic solar proton events in the upper stratosphere and, approaching solar minimum conditions, a slowly increasing flux of cosmic rays.

To include ionization by electrons a much more complex calculation is necessary, as electron flux is much more dependent on the state of the magnetosphere and the radiation belts. We therefore used the AIMOS data set to include ionization caused by electrons, see the corresponding Chap. 13 of J.M. Wissing and M. Kallenrode. Additional to precipitating electrons, this data-set also considers protons and α-Particles, based on measured particle fluxes. We applied both data sets for the solar proton event in Oct/Nov 2003, and found better agreement of observed and simulated NO_x when applying our module. With the limitations of the observations of the particle flux and other assumptions to derive a energy flux spectrum, this underlines that more detailed observations of incoming particle fluxes are necessary.

15.3.2 Model Intercomparison

The SP event in Oct/Nov 2003 is an ideally suited testbed for simulations of direct effects in the middle atmosphere caused by energetic particles as the detailed observations of the MIPAS instrument allow to validate the response of all the most important chemical species in the models. MIPAS showed changes after the event for species such as NO, NO_2, H_2O_2, O_3, N_2O, HNO_3, N_2O_5, HNO_4, ClO, HOCl, and $ClONO_2$. The HEPPA model data intercomparison initiative brought together scientists involved in atmospheric modeling using state-of-the art CCMs and chemistry-transport models on one hand and scientists involved in the analysis and generation of MIPAS IMK/IAA data on the other hand. The objective of this community effort was (i) to assess the ability of state-of-the-art atmospheric models to reproduce

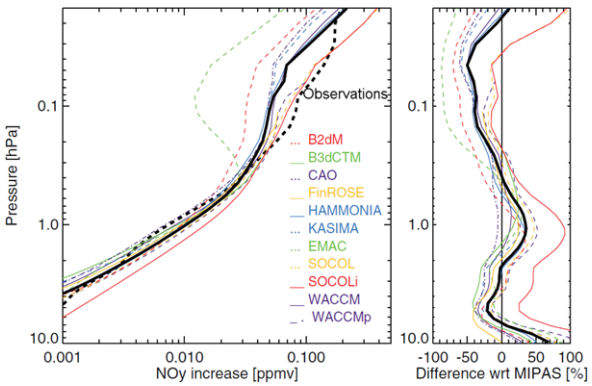

Fig. 15.9 Area-weighted averages (40–90N) of observed and modeled NOy enhancements during 30 October 1 November with respect to 26 October (*left*) and relative deviations of modeled averages from the MIPAS observations (*right*). *Thick solid* and *dashed lines* represent model multi-model mean average and MIPAS observations, respectively. WACCMp denotes the WACCM simulation including proton ionization only (excluded from multi-model-mean) (from *Funke et al.* [2011])

SPE-induced composition changes, (ii) to identify and—if possible—remedy deficiencies in chemical schemes, and (iii) to serve as a platform for discussion between modelers and data producers. This was achieved by a quantitative comparison of observed and modeled species abundances during and after SPEs, as well as by intercomparing the simulations performed by the different models. The initiative focused in its first phase on the inter-comparison of IMK/IAA generated MIPAS/Envisat data obtained in the aftermath of the October/November 2003 SPE with model results.

We give here a few examples of results of the intercomparison for the KASIMA model which extend the studies presented in Sect. 15.2. We refer to the extensive paper of *Funke et al.* [2011] for the complete inter-comparison and the discussion of the results.

An important parameter for subsequent chemical effects caused by the EPP is the amount of additional reactive nitrogen compounds which is produced in the event, expressed as additional NOy. Figure 15.9 shows the observed NOy enhancement and the results of the models directly after the SPE. The agreement seems to be satisfactory, but note the logarithmic scale. As most other models, KASIMA overestimates NOy below about 0.5 hPa and shows some underestimation above. This discrepancy hints to difficulties in describing the ionization rate, see discussion in the section above.

Figure 15.10 top shows the development of CO in observations and the model. Obviously KASIMA overestimates the downward transport compared to observations. A too fast descent in the Northern polar winter stratosphere was also found in the analysis discussed in *Reddmann et al.* [2010]. Figure 15.10 shows an example for substances from the chlorine family. Whereas HOCl changes are well represented in the model, $ClONO_2$ changes are underestimated to a great extent which is probably related to lower ClO values in the models compared to MIPAS even

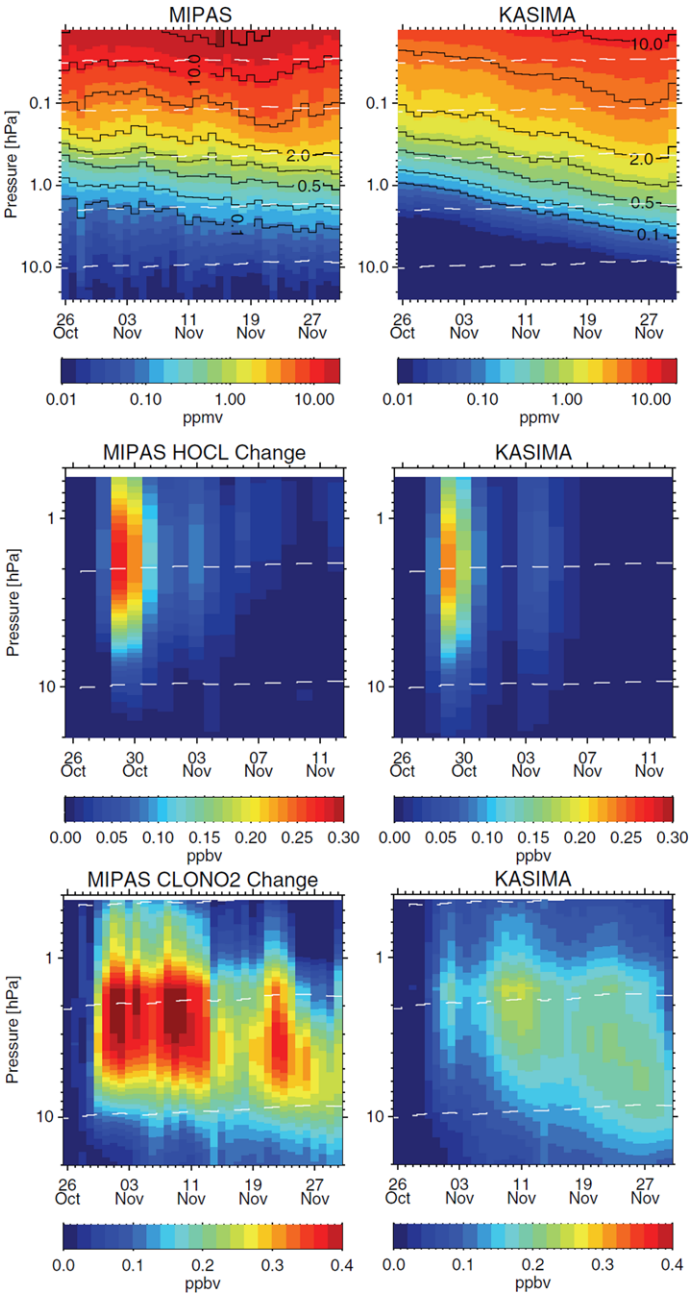

Fig. 15.10 Examples from the HEPPA intercomparison showing KASIMA results. *Top row*: CO time series derived from MIPAS and from KASIMA (ppm). Time series of HOCl and $ClONO_2$ derived from MIPAS observations and difference to KASIMA (ppb)

during background conditions. Other differences between models and observations concern HNO_3 buildup during and shortly after the event, It was shown by *Verronen et al.* [2008] that this is most likely due to missing ion chemistry in most of the models.

15.4 Hydrogen Peroxid as an Indicator for HO_x Production

Besides the production of NO_x, also HO_x is produced in the course of energetic particle precipitation. Changes in trace gases like HOCl, HNO_4 or HNO_3 are dependent on changes in the concentration of the HO_x family. It is therefore worth to try to assess members of the HO_x family directly by observations and to document the changes caused by the EPP. But only the gas H_2O_2, which acts as a reservoir gas for HO_x shows sufficiently strong spectral features in the spectral range of the MIPAS instrument. Therefore, the MIPAS/ENVISAT full and reduced resolution spectra were analyzed to develop a retrieval approach for H_2O_2.

The main source of H_2O_2 is the HO_2 self-reaction:

$$HO_2 + HO_2 \longrightarrow H_2O_2 + O_2 \tag{15.1}$$

Of minor importance is the three-body reaction:

$$OH + OH + M \longrightarrow H_2O_2 + M \tag{15.2}$$

The main sink in the stratosphere is through photolysis:

$$H_2O_2 + h\nu \longrightarrow 2OH \tag{15.3}$$

The reactions with OH and atomic oxygen destroy H_2O_2 to a lesser extent.

15.4.1 Hydrogen Peroxide Spectral Signatures and Retrieval Set-Up

In the mid-infrared spectral region, which is covered by the spectral range of MIPAS, hydrogen peroxide shows weak emission lines between about 1210 cm^{-1} and 1320 cm^{-1} (Fig. 15.11). All these lines belong to the H_2O_2 ν_6 band centered at 1266 cm^{-1}. The spectral signatures are taken from the latest update for H_2O_2 (based on measurements from *Perrin et al.* [1995] and *Klee et al.* [1999]) in the HITRAN 2004 molecular spectroscopic database [*Rothman et al.*, 2005]. The challenge of the hydrogen peroxide retrieval is the very weak signal of the emission lines in comparison to the instrumental noise which is much higher in this spectral region than the H_2O_2 signal (Fig. 15.11).

For the retrieval, 19 narrow spectral regions (microwindows) were selected between 1220 cm^{-1} and 1265 cm^{-1}, which is the lower end of MIPAS channel AB and includes the R-branch of the H_2O_2 ν_6 band. Those microwindows are used up to tangent altitudes of 47 km.

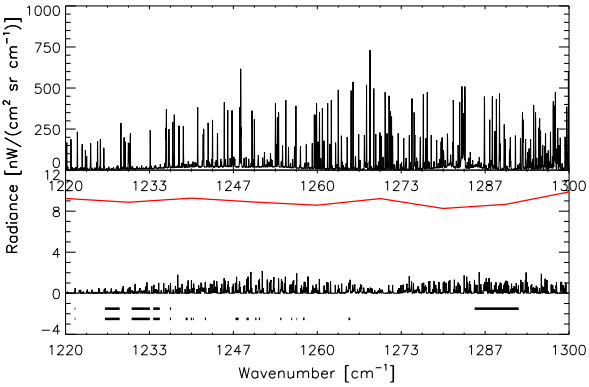

Fig. 15.11 Spectral range of the H_2O_2 ν_6 rotations-vibration band; *Top*: emission of all gases; *Bottom*: emission of H_2O_2 (*black*) and typical noise in MIPAS-spectra (*red*); *black lines* mark used spectral windows, lower row for heights below 44.5 km, top row above (from *Versick* [2011])

The main criterion for the selection was high sensitivity to hydrogen peroxide and low interference by other gases. Unfortunately the P-branch can not be used in the lower stratosphere for our retrieval because the lines of the interfering gases are too dense. Above 47 km an additional microwindow from 1285 cm^{-1} to 1292 cm^{-1} is used. The microwindows between 1237 cm^{-1} and 1265 cm^{-1} are not used in this altitude regions due to potentially bad absorption cross sections for N_2O_5 at low pressures.

Since the hydrogen peroxide contribution is so small, the contribution of other gases still needs to be considered and HOCl, CH_4, N_2O, N_2O_5 and COF_2 have to be retrieved jointly. Other gases had to be retrieved before the hydrogen peroxide retrieval and the results had to be used in our H_2O_2 retrieval. These gases are: H_2O, O_3, $ClONO_2$ and HNO_3. For all the other gases in this spectral region climatological values were used.

The retrieval procedure follows a scheme analog to that described by *Rodgers* [2000]:

$$\begin{aligned}\mathbf{x}_{i+1} = \mathbf{x}_i &+ \left(\mathbf{K}_i^{\mathbf{T}}\mathbf{S}_{\mathbf{y}}^{-1}\mathbf{K}_i + \mathbf{R}\right)^{-1} \\ &\times \left[\mathbf{K}_i^{\mathbf{T}}\mathbf{S}_{\mathbf{y}}^{-1}\left(\mathbf{y} - \mathbf{F}(\mathbf{x}_i)\right) - \mathbf{R}(\mathbf{x}_i - \mathbf{x_a})\right] \end{aligned} \tag{15.4}$$

where $\mathbf{x}$ is the retrieval vector, $\mathbf{K}$ the partial derivatives of the spectral grid points with respect to the retrieval vector (Jacobian), $\mathbf{S_y}$ the covariance matrix due to the measurement noise, $\mathbf{R}$ the regularization or constraint matrix, $\mathbf{y}$ the measurement vector, $\mathbf{F}$ the forward model, $\mathbf{x_a}$ the a priori profile, and i the iteration index.

Due to the very high noise in comparison to the signal we had to choose a rather high regularization strength giving us a low number of degrees of freedom. The regularization is stronger in the upper stratosphere. It is weakest in the middle stratosphere where we expect the maximum volume mixing ratio of H_2O_2. Lowest measurements used were around 25 km because otherwise oscillations in our profiles occurred due to error propagation from below which caused subsequent faults in other altitudes. The retrieval setup was verified by retrieval of H_2O_2 from synthetic spectra. These spectra were calculated with the Karlsruhe optimized and Precise Radiative transfer Algorithm (KOPRA) [*Stiller*, 2000]. The error analysis showed

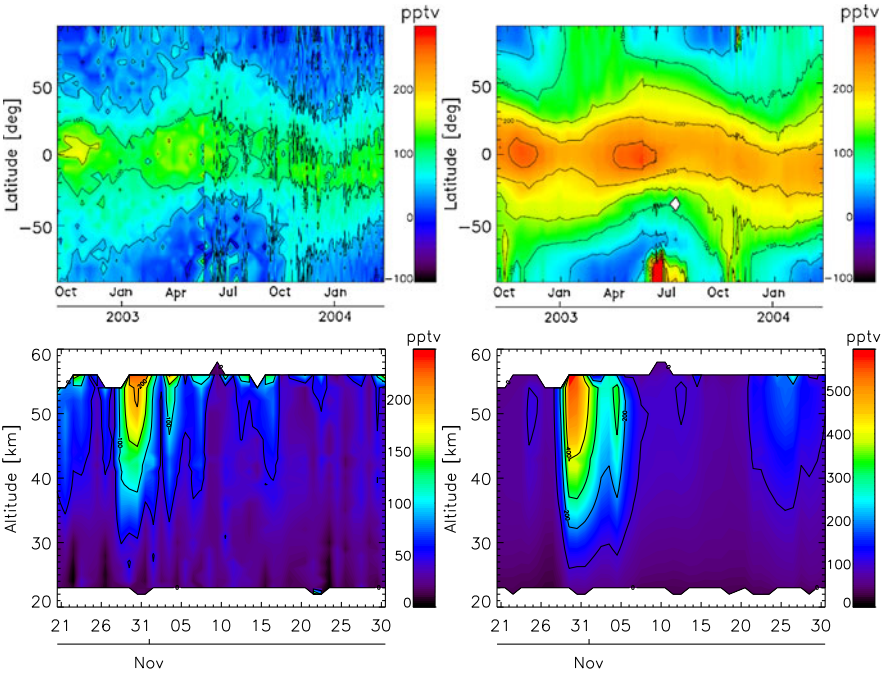

Fig. 15.12 Retrieval (*left*) and model (*right*) results of H_2O_2: top temporal evolution of the daily zonal means at 30 km; KASIMA results are shown on MIPAS geolocations convolved with the MIPAS AK. (*Bottom*): Time-height cross section of H_2O_2 during the Halloween storms; MIPAS averaging kernels has been applied on KASIMA results (from *Versick* [2011])

that concentrations of H_2O_2 can be retrieved between 20–60 km. The corresponding vertical resolution is about 8 km in the lower stratosphere and about 35 km in the upper stratosphere. Comparison of H_2O_2 MIPAS measurements with models must be done by convolving the model results with the MIPAS averaging kernel.

15.4.2 Distribution of H_2O_2 Under Normal and Disturbed Conditions

The temporal evolution of the H_2O_2 stratospheric distribution in KASIMA is very similar to the temporal evolution in the MIPAS measurements (see Fig. 15.12). Both show the highest vmr in the inner tropics shortly after equinox. In the tropics and subtropics the H_2O_2 volume mixing ratio is following the position of the overhead sun. Higher volume mixing ratios are reached in the summer hemisphere. Also the lower volume mixing ratio in the end of 2003 and beginning of 2004 are represented by KASIMA. The absolute value of the mixing ratio vmr in KASIMA is almost twice that of MIPAS. Sensitivity studies show that this could be related to uncertainties of associated reaction rate-constants.

Figure 15.12 shows the temporal evolution of H_2O_2 during the Halloween storms. The retrieval clearly shows enhancements related to the ionization events. The model grossly overestimates the observed concentrations during the SPE. From the HEPPA inter-comparison similar results have been found for other models. Further details of the retrieval procedure and results can be found in *Versick* [2011] and *Versick et al.* [2011].

The reduced resolution mode of MIPAS after March 2004 makes regular observations of H_2O_2 more difficult, and global distributions could not be derived until now. But after the exceptional SP events in January 2005, H_2O_2 enhancements could also be derived in the reduced resolution mode. Together with observations of MLS instrument on the AURA satellite, a more complete characterization of the HO_x family after SPE events was possible (for details see *Jackman et al.*, 2011).

15.5 HNO_3 Enhancements

In the middle stratosphere, the reactive nitrogen compounds NO and NO_2 are converted to reservoir gases, of which HNO_3 is the most abundant. *Orsolini et al.* [2005] found much higher HNO_3 concentrations observed by MIPAS/ENVISAT when compared to their model for the winter 2003/2004, *Stiller et al.* [2005] analyzed the Antarctic winter 2003, when a distinct secondary maximum of HNO_3 was found in MIPAS/ENVISAT data at about 40 km. These observations are in line with findings from earlier satellite missions [*Austin et al.*, 1986; *Kawa et al.*, 1995]. The latter explained this discrepancy as a result of reactions of N_2O_5 with water cluster ions. This reaction, originally proposed by *Böhringer et al.* [1983], had been combined with heterogeneous reactions on sulfate aerosols by *de Zafra and Smyshlyaev* [2001] in order to understand HNO_3 satellite and ground based observations in polar winters.

First comparisons of the HNO_3 observations with the KASIMA model also showed a pronounced underestimation of HNO_3 in the late polar winter when high NO_x concentrations indicate strong NO_x intrusions. We therefore included the parameterization of *de Zafra and Smyshlyaev* [2001] in our chemistry module and got reasonable agreement with the observations (see *Reddmann et al.* [2010]).

The parameterization of *de Zafra and Smyshlyaev* [2001] uses a fixed profile for protonized water clusters. Using a formulation for the cluster concentration according to *Aplin and McPheat* [2005] a variant of this parameterization was developed where the concentration of water clusters is dependent on the actual ionization rate. Figure 15.13 compares versions of the KASIMA model with no additional conversion, the implementation of *de Zafra and Smyshlyaev* [2001] and the new approach. The conversion to HNO_3 is strongest in the new version, and results in too low N_2O_5 concentrations compared to the MIPAS results. Interestingly, through the ionization by cosmic rays we found a pronounced effect of this reaction in the lower stratosphere, bringing the regular maximum of HNO_3 at about 25 km in closer agreement to the observations.

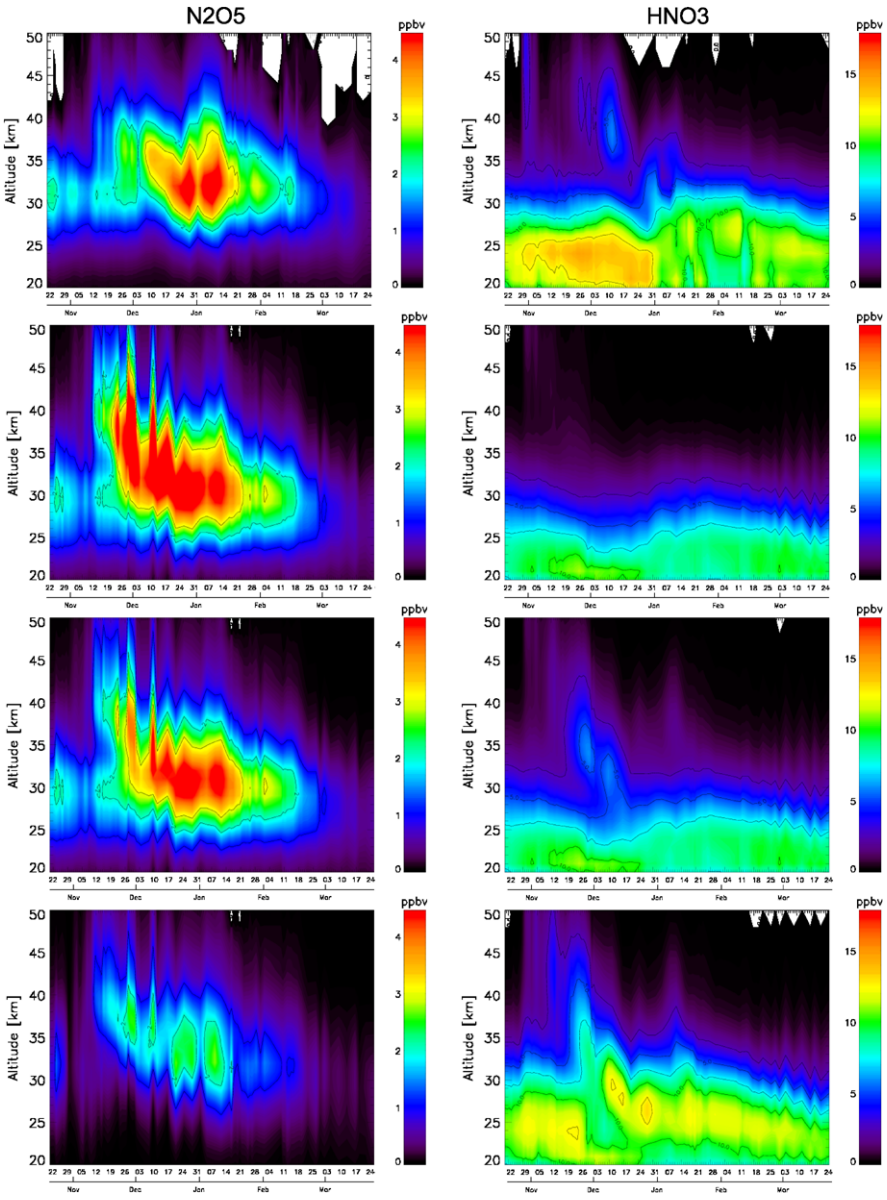

Fig. 15.13 N_2O_5 and HNO_3 time-height cross sections for the Arctic winter 2003/4. From top MIPAS observations, KASIMA simulations without reaction with protonized water clusters, KASIMA including the reaction parameterized according *de Zafra and Smyshlyaev* [2001], and reaction with ionization rate dependent concentration of water clusters

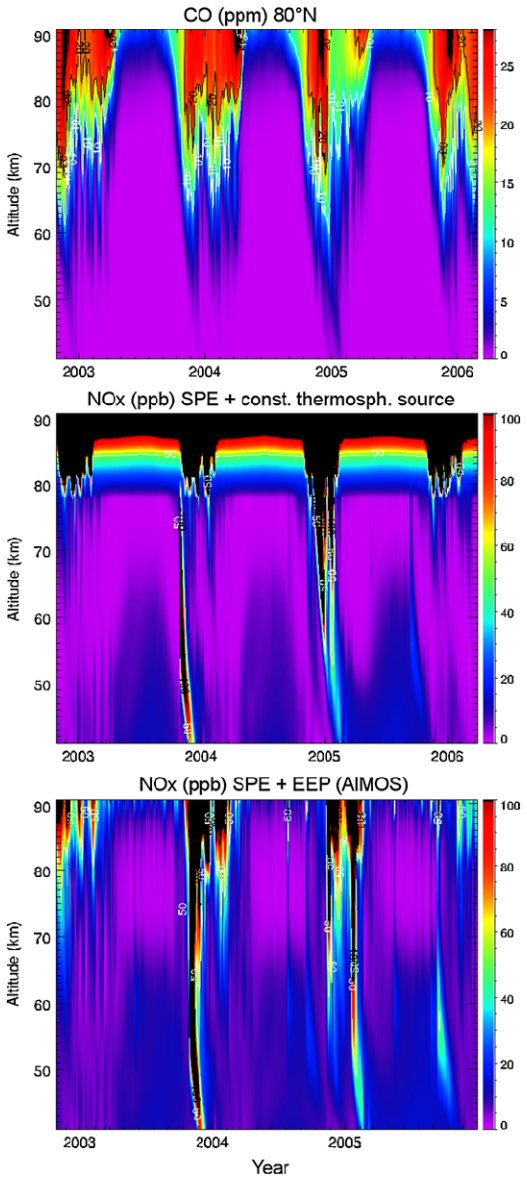

Fig. 15.14 KASIMA simulations of the NH winters 2002/3–2005/6. CO serves as an upper mesospheric tracer, the artificial thermospheric NO_x probes possible transport from the lower thermosphere, and the simulation including the AIMOS electron component probes possible ionization in the mesosphere from auroral sources. The winter 2003/4 and 2006/7 with observed strong intrusion are marked

15.6 The Question of the Origin of NO_x Intrusions

In winter 2003/4 the analysis showed that it is not the SPE which caused most of long-term impacts on ozone but the NO_x enhancements transported from above about 80 km. The question where the massive NO_x intrusions observed in the Arctic winter 2003/4 (see Sect. 15.2), 2005/6 and 2008/9 have its origin is currently under debate. Figure 15.14 shows output of a KASIMA simulation where the downward

transport and ionization via electrons is probed. The model shows especially for the 2003/4 and 2005/6 no pronounced downward transport for CO, here used as a tracer for mesospheric air masses. This agrees with the fact that also an artificial thermospheric NO_x source in the model does not contribute to massive NO_x enhancements in contrast to the observations. But also the inclusion of auroral electron ionization according precalculated ionization rates through the AIMOS model does not improve this deviation from observations. Many models seem to fail to simulate the massive NO_x enhancements but it is not clear for what reasons. It was suggested that due to the limited energy range and resolution of the particle counters, precipitation of highly relativistic electrons might not be detected. The fact that the massive enhancements observed in the past Arctic winters occurred after strong stratospheric warmings and accompanied by an elevated stratopause *Smith et al.* [2009] strongly suggests however, that dynamical processes as the propagation of gravity waves play an important role, as the propagation of gravity waves. As it is well known that gravity wave drag is represented in models only in a parameterized form, a plausible reason for the failure of the model is some deficit in the representation of processes connected to gravity waves and their deposition of energy and momentum. Further model studies and observations, specifically in the MLT region are necessary to solve this question.

References

Aplin, K., & McPheat, R. (2005). Absorption of infra-red radiation by atmospheric molecular cluster-ions. *Journal of Atmospheric and Solar-Terrestrial Physics*, *67*(8–9), 775–783. doi:10.1016/j.jastp.2005.01.007. 1st General Meeting of the European-Geosciences-Union, Nice, France, Apr 25, 2004.

Austin, J., Garcia, R. R., Russell III, J. M., Solomon, S., & Tuck, A. F. (1986). On the atmospheric photochemistry of nitric acid. *Journal of Geophysical Research*, *91*, 5477–5485.

Baumgaertner, A. J. G., Joeckel, P., & Bruehl, C. (2009). Energetic particle precipitation in ECHAM5/MESSy1-Part 1: downward transport of upper atmospheric NOx produced by low energy electrons. *Atmospheric Chemistry and Physics*, *9*(8), 2729–2740.

Böhringer, H., Fahey, D. W., Fehsenfeld, F. C., & Ferguson, E. E. (1983). The role of ion-molecule reactions in the conversion of N_2O_5 to HNO_3 in the stratosphere. *Planetary and Space Science*, *31*, 185–191. doi:10.1016/0032-0633(83)90053-3.

Brasseur, G. P., & Solomon, S. (2005). *Aeronomy of the middle atmosphere*. Berlin: Springer.

Callis, L., Baker, D., Natarajan, M., Blake, J., Mewaldt, R., Selesnick, R., & Cummings, J. (1996). A 2-D model simulation of downward transport of NOy into the stratosphere: effects on the 1994 austral spring O_3 and NOy. *Geophysical Research Letters*, *23*(15), 1905–1908.

Carli, B., Alpaslan, D., Carlotti, M., Castelli, E., Ceccherini, S., Dinelli, B. M., Dudhia, A., Flaud, J. M., Hoepfner, M., Jay, V., Magnani, L., Oelhaf, H., Payne, V., Piccolo, C., Prosperi, M., Raspollini, P., Remedios, J., Ridolfi, M., & Spang, R. (2004). First results of MIPAS/ENVISAT with operational level 2 code. *Advances in Space Research*, *33*(7), 1012–1019.

de Zafra, R., & Smyshlyaev, S. (2001). On the formation of HNO3 in the Antarctic mid to upper stratosphere in winter. *Journal of Geophysical Research*, *106*(D19), 23115–23125.

Engel, A., Mobius, T., Haase, H. P., Bonisch, H., Wetter, T., Schmidt, U., Levin, I., Reddmann, T., Oelhaf, H., Wetzel, G., Grunow, K., Huret, N., & Pirre, M. (2006). Observation of mesospheric air inside the arctic stratospheric polar vortex in early 2003. *Atmospheric Chemistry and Physics*, *6*, 267–282.

Fischer, H., & Oelhaf, H. (1996). Remote sensing of vertical profiles of atmospheric trace constituents with MIPAS limb-emission spectrometers. *Applied Optics*, *35*(16), 2787–2796.

Fischer, H., Birk, M., Blom, C., Carli, B., Carlotti, M., von Clarmann, T., Delbouille, L., Dudhia, A., Ehhalt, D., Endemann, M., Flaud, J. M., Gessner, R., Kleinert, A., Koopman, R., Langen, J., Lopez-Puertas, M., Mosner, P., Nett, H., Oelhaf, H., Perron, G., Remedios, J., Ridolfi, M., Stiller, G., & Zander, R. (2008). MIPAS: an instrument for atmospheric and climate research. *Atmospheric Chemistry and Physics*, *8*(8), 2151–2188.

Funke, B., Lopez-Puertas, M., von Clarmann, T., Stiller, G. P., Fischer, H., Glatthor, N., Grabowski, U., Hopfner, M., Kellmann, S., Kiefer, M., Linden, A., Tsidu, G. M., Milz, M., Steck, T., & Wang, D. Y. (2005). Retrieval of stratospheric nox from 5.3 and 6.2 µm nonlocal thermodynamic equilibrium emissions measured by Michelson interferometer for passive atmospheric sounding (MIPAS) on envisat. *Journal of Geophysical Research. Atmospheres*, *110*(D9), D09302.

Funke, B., López-Puertas, M., Fischer, H., Stiller, G., von Clarmann, T., Wetzel, G., Carli, B., & Belotti, C. (2007). Comment on "origin of the January-April 2004 increase in stratospheric NO_2 observed in northern polar latitudes" by Jean-Baptist Renard et al. *Geophysical Research Letters*, *34*, 107813. doi:10.1029/2006GL027518.

Funke, B., López-Puertas, M., García-Comas, M., Stiller, G. P., von Clarmann, T., & Glatthor, N. (2008). Mesospheric N_2O enhancements as observed by MIPAS on Envisat during the polar winters in 2002–2004. *Atmospheric Chemistry and Physics*, *8*, 5787–5800.

Funke, B., Baumgaertner, A., Calisto, M., Egorova, T., Jackman, C. H., Kieser, J., Krivolutsky, A., López-Puertas, M., Marsh, D. R., Reddmann, T., Rozanov, E., Salmi, S.-M., Sinnhuber, M., Stiller, G. P., Verronen, P. T., Versick, S., von Clarmann, T., Vyushkova, T. Y., Wieters, N., & Wissing, J. M. (2011). Composition changes after the "halloween" solar proton event: the high-energy particle precipitation in the atmosphere (heppa) model versus MIPAS data intercomparison study. *Atmospheric Chemistry and Physics Discussions*, *11*(3), 9407–9514. doi:10.5194/acpd-11-9407-2011.

Funke, B., Lopez-Puertas, M., Gil-Lopez, S., von Clarmann, T., Stiller, G., Fischer, H., & Kellmann, S. (2005). Downward transport of upper atmospheric NOx into the polar stratosphere and lower mesosphere during the Antarctic 2003 and Arctic 2002/2003 winters. *Journal of Geophysical Research*, *110*(D24). doi:10.1029/2005JD006463.

Grooß, J.-U., Konopka, P., & Müller, R. (2005). Ozone chemistry during the 2002 Antarctic vortex split. *Journal of the Atmospheric Sciences*, *62*(3), 860–870.

Heaps, M. (1978). Parameterization of cosmic-ray ion-pair production-rate above 18 km. *Planetary and Space Science*, *26*(6), 513–517.

Jackman, C., & McPeters, R. (2004). The effects of solar proton events on ozone and other constituents. *Geophysical Monograph*, *141*, 305–319.

Jackman, C. H., DeLand, M. T., Labow, G. J., Fleming, E. L., Weisenstein, D. K., Ko, M. K. W., Sinnhuber, M., & Russell, J. M. (2005). Neutral atmospheric influences of the solar proton events in October-November 2003. *Journal of Geophysical Research*, *110*(A9), A09S27.

Jackman, C. H., Marsh, D. R., Vitt, F. M., Roble, R. G., Randall, C. E., Bernath, P. F., Funke, B., López-Puertas, M., Versick, S., Stiller, G. P., Tylka, A. J., & Fleming, E. L. (2011). Northern hemisphere atmospheric influence of the solar proton events and ground level enhancement in January 2005. *Atmospheric Chemistry and Physics Discussion*, *11*(3), 7715–7755. doi:10.5194/acpd-11-7715-2011.

Jackman, C. H., Marsh, D. R., Vitt, F. M., Garcia, R. R., Fleming, E. L., Labow, G. J., Randall, C. E., Lopez-Puertas, M., Funke, B., von Clarmann, T., & Stiller, G. P. (2008). Short- and medium-term atmospheric constituent effects of very large solar proton events. *Atmospheric Chemistry and Physics*, *8*(3), 765–785.

Kawa, S. R., Kumer, J. B., Douglass, A. R., Roche, A. E., Smith, S. E., Taylor, F. W., & Allen, D. J. (1995). Missing chemistry of reactive nitrogen in the upper stratospheric polar winter. *Geophysical Research Letters*, *22*, 2629–2632. doi:10.1029/95GL02336.

Khosrawi, F., Mueller, R., Proffitt, M. H., Ruhnke, R., Kirner, O., Joeckel, P., Grooss, J. U., Urban, J., Murtagh, D., & Nakajima, H. (2009). Evaluation of CLaMS, KASIMA and

ECHAM5/MESSy1 simulations in the lower stratosphere using observations of Odin/SMR and ILAS/ILAS-II. *Atmospheric Chemistry and Physics*, *9*(15), 5759–5783.

Klee, S., Winnewisser, M., Perrin, A., & Flaud, J.-M. (1999). Absolute line intensities for the ν_6 band of H_2O_2. *Journal of Molecular Spectroscopy*, *195*, 154–161.

Konopka, P., Grooß, J. U., Günther, G., McKenna, D. S., Müller, R., Elkins, J. W., Fahey, D., & Popp, P. (2003). Weak impact of mixing on chlorine deactivation during SOLVE/THESEO2000: Lagrangian modeling (CLaMS) versus ER-2 in situ observations. *Journal of Geophysical Research*, *108*, 8324. doi:10.1029/2001JD000876.

Konopka, P., Steinhorst, H.-M., Grooß, J.-U., Günther, G., Müller, R., Elkins, J. W., Jost, H.-J., Richard, E., Schmidt, U., Toon, G., & McKenna, D. S. (2004). Mixing and ozone loss in the 1999–2000 Arctic vortex: simulations with the 3-dimensional chemical Lagrangian model of the stratosphere (CLaMS). *Journal of Geophysical Research*, *109*, D02315. doi:10.1029/2003JD003792.

Konopka, P., Günther, G., Müller, R., dos Santos, F. H. S., Schiller, C., Ravegnani, F., Ulanovsky, A., Schlager, H., Volk, C. M., Viciani, S., Pan, L. L., McKenna, D.-S., & Riese, M. (2007a). Contribution of mixing to upward transport across the tropical tropopause layer (TTL). *Atmospheric Chemistry and Physics*, *7*(12), 3285–3308.

Konopka, P., Engel, A., Funke, B., Müller, R., Grooß, J.-U., Günther, G., Wetter, T., Stiller, G., von Clarmann, T., Glatthor, N., Oelhaf, H., Wetzel, G., López-Puertas, M., Pirre, M., Huret, N., & Riese, M. (2007b). Ozone loss driven by nitrogen oxides and triggered by stratospheric warmings may outweigh the effect of halogens. *Journal of Geophysical Research*, *112*, D05105. doi:10.1029/2006JD007064.

Kouker, W. (1993). Evaluation of dynamical parameters with a 3-D mechanistic model of the middle atmosphere. *Journal of Geophysical Research*, *98*, 23165–23191.

Kouker, W., Offermann, D., Kull, V., Ruhnke, R., Reddmann, T., & Franzen, A. (1999). Streamers observed by the CRISTA experiment and simulated in the KASIMA model. *Journal of Geophysical Research*, *104*, 16405–16418.

Lacoste-Francis, H. (Ed.) (2010). *MIPAS observations of stratospheric and upper tropospheric trace gases: an overview: Vol. ESA SP-686*. CD-ROM. ESA Publications Division, ESTEC, Postbus 299, 2200 AG Noordwijk, The Netherlands.

Langematz, U., Grenfell, J., Matthes, K., Mieth, P., Kunze, M., Steil, B., & Bruhl, C. (2005). Chemical effects in 11-year solar cycle simulations with the Freie Universität Berlin climate middle atmosphere model with online chemistry (FUB-CMAM-CHEM). *Geophysical Research Letters*, *32*(13). doi:10.1029/2005GL022686.

Lopez-Puertas, M., Funke, B., Gil-Lopez, S., von Clarmann, T., Stiller, G. P., Hopfner, M., Kellmann, S., Fischer, H., & Jackman, C. H. (2005a). Observation of nox enhancement and ozone depletion in the northern and southern hemispheres after the October-November 2003 solar proton events. *Journal of Geophysical Research*, *110*(A9), A09S43.

Lopez-Puertas, M., Funke, B., Gil-Lopez, S., von Clarmann, T., Stiller, G. P., Hopfner, M., Kellmann, S., Tsidu, G. M., Fischer, H., & Jackman, C. H. (2005b). HNO_3, N_2O_5, and $ClONO_2$ enhancements after the October-November 2003 solar proton events. *Journal of Geophysical Research*, *110*(A9), A09S44.

McKenna, D. S., Konopka, P., Grooß, J.-U., Günther, G., Müller, R., Spang, R., Offermann, D., & Orsolini, Y. (2002a). A new chemical Lagrangian model of the stratosphere (CLaMS): 1. Formulation of advection and mixing. *Journal of Geophysical Research*, *107*(D16), 4309. doi:10.1029/2000JD000114.

McKenna, D. S., Grooß, J.-U., Günther, G., Konopka, P., Müller, R., Carver, G., & Sasano, Y. (2002b). A new chemical Lagrangian model of the stratosphere (CLaMS): 2. Formulation of chemistry scheme and initialization. *Journal of Geophysical Research*, *107*(D15), 4256. doi:10.1029/2000JD000113.

Orsolini, Y. J., Manney, G. L., Santee, M. L., & Randall, C. E. (2005). An upper stratospheric layer of enhanced hno3 following exceptional solar storms. *Geophysical Research Letters*, *32*(12), L12S01.

Perrin, A., Valentin, A., Flaud, J.-M., Camy-Peyret, C., Schriver, L., Schriver, A., & Arcas, P. (1995). The 7.9-μm band of hydrogen peroxide: line positions and intensities. *Journal of Molecular Spectroscopy*, *171*, 358–373.

Randall, C., Siskind, D., & Bevilacqua, R. (2001). Stratospheric NO_x enhancements in the southern hemisphere vortex in winter/spring 2000. *Geophysical Research Letters*, *28*, 2385–2388.

Randall, C., Rusch, D., Bevilacqua, R., Hoppel, K., & Lumpe, J. (1998). Polar ozone and aerosol measurement (POAM) II stratospheric NO_2, 1993–1996. *Journal of Geophysical Research*, *103*(D21), 28361–28371.

Randall, C. E., Harvey, V. L., Singleton, C. S., Bailey, S. M., Bernath, P. F., Codrescu, M., Nakajima, H., & Russell, J. M. (2007). Energetic particle precipitation effects on the southern hemisphere stratosphere in 1992–2005. *Journal of Geophysical Research*, *112*(D11), 8308. doi:10.1029/2006JD007696.

Reddmann, T., Ruhnke, R., & Kouker, W. (1999). Use of coupled ozone fields in a 3-D circulation model of the middle atmosphere. *Annales Geophysicae*, *17*, 415–429.

Reddmann, T., Ruhnke, R., & Kouker, W. (2001). Three-dimensional model simulations of SF_6 with mesospheric chemistry. *Journal of Geophysical Research*, *106*, 14525–14537.

Reddmann, T., Ruhnke, R., Versick, S., & Kouker, W. (2010). Modeling disturbed stratospheric chemistry during solar-induced NOx enhancements observed with MIPAS/ENVISAT, *Journal of Geophysical Research*, *115*. doi:10.1029/2009JD012569.

Ridolfi, M., Carli, B., Carlotti, M., von Clarmann, T., Dinelli, B. M., Dudhia, A., Flaud, J. M., Hopfner, M., Morris, P. E., Raspollini, P., Stiller, G., & Wells, R. J. (2000). Optimized forward model and retrieval scheme for mipas near-real-time data processing. *Applied Optics*, *39*(8), 1323–1340.

Rinsland, C. E. A. (1996). ATMOS measurements of $H_2O + 2CH_4$ and total reactive nitrogen in the November 1994 Antarctic stratosphere: dehydration and denitrification in the vortex. *Geophysical Research Letters*, *23*, 2397–2400.

Rodgers, C. D. (2000). Inverse methods for atmospheric sounding: theory and practice. In F. W. Taylor (Ed.), *Series on atmospheric: Vol. 2. Oceanic and planetary physics* (p. 238), Singapore: World Scientific.

Rothman, L. S., Jacquemart, D., Barbe, A., Benner, D. C., Birk, M., Brown, L. R., Carleer, M. R., Chackerian Jr., C., Chance, K., Coudert, L. H., Dana, V., Devi, V. M., Flaud, J.-M., Gamache, R. R., Goldman, A., Hartmann, J.-M., Jucks, K. W., Maki, A. G., Mandin, J.-Y., Massie, S. T., Orphal, J., Perrin, A., Rinsland, C. P., Smith, M. A. H., Tennyson, J., Tolchenov, R. N., Toth, R. A., Vander Auwera, J., Varanasi, P., & Wagner, G. (2005). The HITRAN 2004 molecular spectroscopic database. *Journal of Quantitative Spectroscopy & Radiative Transfer*, *96*, 139–204.

Rozanov, E., Callis, L., Schlesinger, M., Yang, F., Andronova, N., & Zubov, V. (2005). Atmospheric response to NOy source due to energetic electron precipitation. *Geophysical Research Letters*, *32*(14). doi:10.1029/2005GL023041.

Ruhnke, R., Kouker, W., & Reddmann, T. (1999). The influence of the $OH + NO_2 + M$ reaction on the NO_y partitioning in the late Arctic winter 1992/1993 as studied with KASIMA. *Journal of Geophysical Research*, *104*, 3755–3772.

Sander, S. P., Friedl, R. R., Golden, D. M., Kurylo, M. J., Moortgat, G. K., Keller-Rudek, H., Wine, P. H., Ravishankara, A. R., Kolb, C. E., Molina, M. J., Finlayson-Pitts, B. J., Huie, R. E., & Orkin, V. L. (2006). *Chemical kinetics and photochemical data for use in atmospheric studies* (JPL Publication 06-2).

Siskind, D., Nedoluha, G., Randall, C., Fromm, M., & Russell III, J. (2000). An assessment of southern hemispheric stratospheric NO_x enhancements due to transport from the upper atmosphere. *Geophysical Research Letters*, *27*, 329–332.

Smith, A. K., Lopez-Puertas, M., Garcia-Comas, M., & Tukiainen, S. (2009). SABER observations of mesospheric ozone during NH late winter 2002–2009. *Geophysical Research Letters*, *36*. doi:10.1029/2009GL040942.

Stiller, G. P. (Ed.) (2000). *The Karlsruhe optimized and precise radiative transfer algorithm (KOPRA). Wissenschaftliche Berichte: Vol. FZKA 6487*. Forschungszentrum Karlsruhe.

Stiller, G. P., Tsidu, G. M., von Clarmann, T., Glatthor, N., Hopfner, M., Kellmann, S., Linden, A., Ruhnke, R., Fischer, H., Lopez-Puertas, M., Funke, B., & Gil-Lopez, S. (2005). An enhanced HNO_3 second maximum in the Antarctic midwinter upper stratosphere 2003. *Journal of Geophysical Research*, *110*(D20), D20303.

Stiller, G. P., von Clarmann, T., Hoepfner, M., Glatthor, N., Grabowski, U., Kellmann, S., Kleinert, A., Linden, A., Milz, M., Reddmann, T., Steck, T., Fischer, H., Funke, B., Lopez-Puertas, M., & Engel, A. (2008). Global distribution of mean age of stratospheric air from MIPAS SF_6 measurements. *Atmospheric Chemistry and Physics*, *8*(3), 677–695.

Verronen, P. T., Seppala, A., Kyrola, E., Tamminen, J., Pickett, H. M., & Turunen, E. (2006). Production of odd hydrogen in the mesosphere during the January 2005 solar proton event. *Geophysical Research Letters*, *33*(24). doi:10.1029/2006GL028115.

Verronen, P. T., Funke, B., Lopez-Puertas, M., Stiller, G. P., von Clarmann, T., Glatthor, N., Enell, C. F., Turunen, E., & Tamminen, J. (2008). About the increase of HNO_3 in the stratopause region during the Halloween 2003 solar proton event. *Geophysical Research Letters*, *35*(20). doi:10.1029/2008GL035312.

Versick, S. (2011). *Ableitung von H_2O_2 aus MIPAS/ENVISAT-Beobachtungen und Untersuchung der Wirkung von energetischen Teilchen auf den chemischen Zustand der mittleren Atmosphäre*. Ph.D. thesis, Karlsruher Institut für Technologie.

Versick, S., Stiller, G., von Clarmann, T., Reddmann, T., Glatthor, N., Grabowski, U., Hopfner, M., Kellmann, S., Kiefer, M., Linden, A., Ruhnke, R., & Fischer, H. (2011). Global stratospheric hydrogen peroxide distribution from mipas-envisat full resolution spectra compared to kasima model results. doi:10.5194/acp-12-4923-2012.

Vogel, B., Konopka, P., Grooß, J.-U., Müller, R., Funke, B., López-Puertas, M., Reddmann, T., Stiller, G., von Clarmann, T., & Riese, M. (2008). Model simulations of stratospheric ozone loss caused by enhanced mesospheric NO_x during Arctic Winter 2003/2004. *Atmospheric Chemistry and Physics*, *8*(17), 5279–5293.

von Clarmann, T., Glatthor, N., Hopfner, M., Kellmann, S., Ruhnke, R., Stiller, G. P., Fischer, H., Funke, B., Gil-Lopez, S., & Lopez-Puertas, M. (2005). Experimental evidence of perturbed odd hydrogen and chlorine chemistry after the October 2003 solar proton events. *Journal of Geophysical Research*, *110*(A9), A09S45.

von Clarmann, T., Hoepfner, M., Kellmann, S., Linden, A., Chauhan, S., Funke, B., Grabowski, U., Glatthor, N., Kiefer, M., Schieferdecker, T., Stiller, G. P., & Versick, S. (2009). Retrieval of temperature, H_2O, O_3, HNO_3, CH_4, N_2O, $ClONO_2$ and ClO from MIPAS reduced resolution nominal mode limb emission measurements. *Atmospheric Measurement Techniques*, *2*(1), 159–175.

Wetzel, G., Bracher, A., Funke, B., Goutail, F., Hendrick, F., Lambert, J.-C., Mikuteit, S., Piccolo, C., Pirre, M., Bazureau, A., Belotti, C., Blumenstock, T., de Mazière, M., Fischer, H., Huret, N., Ionov, D., López-Puertas, M., Maucher, G., Oelhaf, H., Pommereau, J.-P., Ruhnke, R., Sinnhuber, M., Stiller, G., van Roozendael, M., & Zhang, G. (2007). Validation of MIPAS-ENVISAT NO_2 operational data. *Atmospheric Chemistry & Physics*, *7*, 3261–3284.

Wissing, J. M., & Kallenrode, M. B. (2009). Atmospheric Ionization Module Osnabruck (AIMOS): a 3-D model to determine atmospheric ionization by energetic charged particles from different populations. *Journal of Geophysical Research*, *114*. doi:10.1029/2008JA013884.